Effects of argon plasma treatment on the osteoconductivity of bone grafting materials

Clinical Oral Investigations

Effects of Argon Plasma treatment on the osteoconductivity of bone grafting materials

--Manuscript Draft--

Manuscript Number:	
Full Title:	Effects of Argon Plasma treatment on the osteoconductivity of bone grafting materials
Article Type:	Original Article
Corresponding Author:	Luigi Canullo, PhD Istituto Stomatologico Toscano Rome, ITALY
Corresponding Author Secondary Information:	
Corresponding Author's Institution:	Istituto Stomatologico Toscano
Corresponding Author's Secondary Institution:	
First Author:	Luigi Canullo, PhD
First Author Secondary Information:	
Order of Authors:	Luigi Canullo, PhD
	Tullio Genova
	Mia Rakic
	Anton Sculean
	Richard Miron
	Maurizio Muzzi
	Stefano Carossa
	Federico Mussano
Order of Authors Secondary Information:	
Funding Information:	
Abstract:	Background The osteoconductive properties of bone grafting materials represent one area of research for the management of bony defects found in the fields of periodontology and oral surgery. From a physico-chemical aspect, the wettability of the graft has been demonstrated to be one of the most important factors for new bone formation. It is also well-known that Argon plasma treatment (PAT) and ultraviolet irradiation (UV) may increase the surface wettability and, consequently, improve the regenerative potential of the bone grafts. Therefore, the aim of the present in vitro study was to evaluate the effect of PAT and UV treatment on the osteoconductive potential of various bone grafts. Materials & Methods The following four frequently used bone grafts were selected for this study: synthetic hydroxyapatite (Mg-HA), biphasic calcium phosphate (BCP), cancellous and cortical xenogenic bone matrices (CaBM, CoBM). Sixty-six serially numbered disks 10mm in diameter were used for each graft material and randomly assigned to the following three groups: test 1 (PAT), test 2 (UV) and control (no treatment). Six samples underwent topographic analysis using SEM pre- and post-treatments to evaluate changes in surface topography/characteristics. Additionally, cell adhesion and cell proliferation were evaluated at 2 and 72 hours respectively following incubation in a three-dimensional culture system utilizing a bioreactor. Furthermore, the effects of PAT and UV on immune cells were assessed by measuring the viability of human

	macrophages at 24 hours. Results The topographic analysis showed different initial morphologies of the commercial biomaterials (e.g. Mg-HA and BCP showed flat morphology, BM samples were extremely porous with high roughness). The surface analysis following experimental treatments did not demonstrate topographical difference when compared to controls. Investigation of cells demonstrated that PAT treatment significantly increased cell adhesion of all 4 evaluated bone substitutes, whereas UV failed to show any statistically significant differences. The viability test revealed no differences in terms of macrophage adhesion on any of the tested surfaces. Conclusion Within their limitations, the present results suggest that treatment of various bone grafting materials with PAT appears to enhance the osteoconductivity of bone substitutes in the early stage by improving osteoblast adhesion without concomitantly affecting macrophage viability. Clinical Relevance Treatment of bone grafts with PAT appears to result in faster osseo-integration of the bone grafting materials and may thus favorably influence bone regeneration.
Suggested Reviewers:	Alexandra Stähli alexandra.staehli@zmk.unibe.ch
	James Deschner james.deschner@uni-mainz.de

Effects of Argon Plasma treatment on the osteoconductivity of bone grafting materials

Authors

Luigi Canullo [1] luigicanullo@yahoo.com

Tullio Genova[2] tullio.genova@gmail.com

Mia Rakic[3] mia.rakic@gmail.com

Anton Sculean[4] anton.sculean@zmk.unibe.ch

Richard Miron[4] richard.miron@zmk.unibe.ch

Maurizio Muzzi[5] maurizio.muzzi@uniroma3.it

Stefano Carossa[2] stefano.carossa@unito.it

Federico Mussano[2] federico.mussano@unito.it

1. Private practice, Rome, Italy
2. CIR Dental School, Department of Surgical Sciences, University of Turin, Italy
3. Nantes University, Department of Periodontology, Nantes, France
4. Department of Periodontology, School of Dental Medicine, University of Bern, Switzerland
5. Department of Science, University Roma Tre, Viale G. Marconi, 446, 00146 Rome, Italy b Laboratorio Interdipartimentale di Microscopia Elettronica (LIME), University Roma Tre

Corresponding Author

Luigi Canullo, Via Nizza, 46 – 00198 Rome, Italy

Phone +39 347 6201976

Email: luigicanullo@yahoo.com

Abstract

Background: The osteoconductive properties of bone grafting materials represent one area of research for the management of bony defects found in the fields of periodontology and oral surgery. From a physico-chemical aspect, the wettability of the graft has been demonstrated to be one of the most important factors for new bone formation. It is also well-known that Argon plasma treatment (PAT) and ultraviolet irradiation (UV) may increase the surface wettability and, consequently, improve the regenerative potential of the bone grafts. Therefore, the aim of the present *in vitro* study was to evaluate the effect of PAT and UV treatment on the osteoconductive potential of various bone grafts.

Materials & Methods: The following four frequently used bone grafts were selected for this study: synthetic hydroxyapatite (Mg-HA), biphasic calcium phosphate (BCP), cancellous and cortical xenogenic bone matrices (CaBM, CoBM). Sixty-six serially numbered disks 10mm in diameter were used for each graft material and randomly assigned to the following three groups: test 1 (PAT), test 2 (UV) and control (no treatment). Six samples underwent topographic analysis using SEM pre- and post-treatments to evaluate changes in surface topography/characteristics. Additionally, cell adhesion and cell proliferation were evaluated at 2 and 72 hours respectively following incubation in a three-dimensional culture system utilizing a bioreactor. Furthermore, the effects of PAT and UV on immune cells were assessed by measuring the viability of human macrophages at 24 hours.

Results: The topographic analysis showed different initial morphologies of the commercial biomaterials (e.g. Mg-HA and BCP showed flat morphology, BM samples were extremely porous with high roughness). The surface analysis following experimental treatments did not demonstrate topographical difference when compared to controls. Investigation of cells demonstrated that PAT treatment significantly increased cell adhesion of all 4 evaluated bone substitutes, whereas UV failed to show any statistically significant differences. The viability test revealed no differences in terms of macrophage adhesion on any of the tested surfaces.

Conclusion: Within their limitations, the present results suggest that treatment of various bone grafting materials with PAT appears to enhance the osteoconductivity of bone substitutes in the early stage by improving osteoblast adhesion without concomitantly affecting macrophage viability.

Clinical Relevance: Treatment of bone grafts with PAT appears to result in faster osseo-integration of the bone grafting materials and may thus favorably influence bone regeneration.

Keywords: bone graft, plasma of Argon, bio-activation, osseointegration, osteoconductivity

Introduction

Bone substitutes/bone grafting materials are frequently used to reconstruct various types of periodontal and bone defects to improve tooth prognosis or accommodate dental implants [1, 2]. The main indications for using bone substitutes are extraction-sockets preservation, as well as lateral/horizontal and vertical bone augmentation [3]. Therefore, filling extraction sockets with slowly-resorbable bone grafts/bone substitutes enables better ridge preservation and improves the conditions for future implant placement [4] Moreover, the use of bone substitutes in conjunction with guided bone regeneration (GBR) is considered a standard treatment modality for lateral bone augmentation, particularly when used in conjunction with implant placement [3]. Furthermore, the use of bone substitute materials provides the stability for immediately placed implants and, by stabilizing soft tissues, contributes also to improvements in aesthetic outcomes [5-7].

Regarding the choice of an ideal bone substitute, a mixture of autogenous bone and synthetic material has previously been suggested in order to reduce the excessive morbidity of the donor site and to compensate for the fast resorption rate of autogenous bone [8, 9]. During lateral augmentations, the additional use of a resorbable membrane has also been recommended to cover the grafts [2]. Similarly, autogenous bone mixed with xenografts and/or alloplastic materials has also been demonstrated efficient for vertical bone regeneration in combination with non-resorbable membranes [10]. In contrast, in case of limited anatomical conditions associated with bone deficiency such as for sinus floor elevation, the use of allografts and xenografts with slower resorbability have been suggested as an optimal choice [11].

Globally, the use of biomaterial-supported reconstructive approaches provides substantially higher clinical improvements in intrabony defects when compared to the open flap debridement (OFD) alone [12]. From a clinical point of view, reconstructive procedures including the use of bone grafting materials, have demonstrated higher clinical attachment level gains, probing depth reductions and defect fill than with OFD alone [13]. However, it was recently emphasized that despite the observed clinical improvement, the clinical and radiographic parameters may not necessarily reflect true histological regeneration [1].

Bone regeneration is a very challenging clinical endeavor since bone cells proliferate substantially slower than fibroblasts and epithelial cells, and thus, bone regeneration can be jeopardized by the ingrowth of non-osseous tissues. Hence, one of the major requests for bone

grafts is the property to maintain the space for the new bone and to prevent fibrous healing [14]. Additionally, differentiation of pre-osteoblasts is regulated by many chemical factors such as partial oxygen pressure and many other signaling factors, indicating that inappropriate local conditions may also negatively affect osseous healing [15]. It has been demonstrated that the healing of bone defects, following the use of bone grafting materials, depends greatly on the interaction between the bone graft and the bone cells of the host, being influenced by the individual bone regenerative potential, defect morphology, and physico-chemical properties of the biomaterial surface [16, 17]. Regarding the physico-chemical surface characteristics of the bone substituents, many factors such as crystallinity, crystal size, particle size, porosity and surface roughness affect the biological behavior of the biomaterial [18]. It has been shown that surface wettability represents the crucial factor for osteoconductivity since the amount of growth factors and proteins on the material particles proportionally increase migration and adhesion of bone cells. In brief, during healing, the bone cells are attracted to the biomaterial surface by the proteins absorbed on the biomaterial surface and further adhere to gradually replace the biomaterial with newly formed bone. The extension and strength of such protein adhesion plays a role in regulating proliferation and differentiation of cells involved in the regeneration process [19]. Highly hydrophilic surfaces have been shown to adsorb these molecules in a denatured and rigid state while highly hydrophobic materials prevent the adsorption of proteins. Moreover, positively charged surfaces have been demonstrated to promote optimal adhesion levels [20].

Irradiation through plasma has become a valuable option among the technologies capable of increasing surface wettability and reactivity of materials [21, 22]. From a physicochemical point of view, the effect of plasma is mediated by the surface activation at the atomic and molecular level, which produces hydrophilic surfaces; thus, enhancing their wettability [23, 24]. In addition, this process has been demonstrated to remove all chemical traces left from former treatments, effectively producing cleaner and better controlled surfaces than with other preparation methods [25, 26]. Consistently, plasma application has been shown to enhance tissue adhesion [27].

Based on these combined previous findings, it was hypothesized that treatments capable of increasing surface wettability may improve the regenerative potential of the bone grafts used in reconstructive surgery of periodontal and bone defects [28]. However, until now limited data are available on the potential influence of PAT and UV treatment on the osteoconductivity of various bone grafts used in reconstructive periodontal and implant surgery [29].

Therefore, the aim of the present *in vitro* study was to evaluate the effect of PAT and UV treatment on the osteoconductivity of bone grafts by assessing osteoblast adhesion and proliferation, surface topography and macrophage adhesion.

Materials and methods

The present *in vitro* study was designed to estimate the effect of two experimental treatments including Argon plasma treatment (PAT) and ultraviolet irradiation (UV) on osteoconductivity of the following four different bone grafts used in reconstructive periodontal and implant surgery:

1. Synthetic pure hydroxyapatite disks (Mg-HA, Sintlife, Finceramica, Faenza Italy)
2. Biphasic calcium phosphate disks (BCP, SUNSTAR Degradable Solutions AG, Schlieren, Switzerland)
3. Cancellous animal bone matrix disks (CaBM, Sp-Block, Tecnoss, Coazze, Italy)
4. Cortical animal bone matrix disks (CoBM, Coritical Lamina, OsteoBiol, Tecnoss, Coazze, Italy)

A power analysis was estimated on the pilot samples [28] using the mean cell adhesion values of 167.7±28.1 cells/field (control) vs 384.5±38.8 cells/field (test) at 2 hours (P =0.0001) will be projected by setting effect size dz = 1.438, error probability a = 0.05, and power = 0.95 (1-b error probability), resulting in 4 samples from each sub-group (G* Power 3.1.7 for Mac OS X Yosemite, version 10.10.3).

Experimental design

The synthetic graft material disks were specially designed for research use within this study. They were pressed from spherical granules and demonstrated a flat surface (size: 600-900 microns for Magnesium-enriched-Hydroxyapatite; size: 450-1000 microns for BCP, made of 60% HA, 40% β-TCP). Xenograft disks (non-commercial products) were produced by trimming from an organic porcine bone maintaining collagen and their porous structure. One-hundred-ten serially numbered blocks 10mm in diameter for each graft material were used in the present study. The blocks were divided into 5 groups of 9 samples each. For each group, four blocks were randomly allocated as test group 1 and underwent Argon plasma treatment (10 W at 1 bar for 20 minutes) in a plasma reactor (Plasma R, Sweden & Martina, Padua, Italy). Additional four graft blocks for each group were allocated as test group 2 and left UV light (Toshiba, Tokyo, Japan) for 20 min (15 W) at ambient conditions (intensity: 0.1 mW/cm2 [λ = 360 ± 20 nm] and 2 mW/cm2 [λ = 250 ± 20 nm]), as described by Aita [30]. The

remaining four graft blocks for each group non-treated disks of each sub-group were used as controls.

Additionally, four samples for each graft material were used for topographic and surface analysis pre- and post-treatment.

A flow diagram is depicted in **Figure 1**.

Cell culture

To characterize the biological response in vitro, two human osteoblast cell lines (MG63, Saos-2, ATCC), macrophages RAW 264.7 (ATCC) and Mesenchymal Stem Cells (D1 ORL-UVA ATCC) were used. Cells were maintained respectively in DMEM 10% Fetal bovine serum (FBS) (Gibco); McCoy's 5a Medium Modified 15% FBS; RPMI-1640 Medium and DMEM 10% FBS adding 100 U/ml penicillin, 100 µg/ml streptomycin, under a humidified atmosphere of 5% CO2 in air, at 37°C. Cells were passaged at sub-confluency to prevent contact inhibition.

Cell adhesion

Cell adhesion on grafts was evaluated using a 24 well plate at 2 hours after plating. Cells were detached using trypsin for 3 minutes, carefully counted and seeded at 2 x 10^3 cells/disk in 100µl of growth medium on the samples. The 24-well plates were kept at 37°C, 0,5%, CO2 for 15 min. The grafts were carefully washed with PBS and were treated with DAPI to stain cell nuclei (Mussano et al. 2017a, Genova et al. 2017) . The number of adherent cells was determined by counting the number of DAPI-positive nuclei.

Bioreactor

In order to obtain a proper cell growth on the graft materials, the LiveBox2 bioreactor (IVTech) was used. The bioreactor is composed of a peristaltic pump, a reservoir and a perfusion chamber. The perfusion chamber is composed of two chambers separated by a porous membrane (**Fig. 2**). The sigmoidal flux mode was implemented so as to achieve a medium flux from the upper chamber to the lower chamber, thus allowing a proper graft perfusion. The bioreactor was kept under a humidified atmosphere of 5% CO_2 in air, at 37°C.

Cell proliferation

To evaluate the effects of PAT and UV treatment on osteoblast proliferation, MG63 and Saos-2 growth was tested by incubating osteoblasts on different graft materials chosen. In order to evaluate the cell proliferation rate, 5000 cells were seeded on each graft sample and incubated for 72h in the bioreactor. Cell proliferation was measured using CellTiter GLO (Promega) following the manufacturer's instructions [31].

Macrophage activation.

Macrophages are widely accepted as regulators of wound healing [32] and play an important role in bone deposition and differentiation of mesenchymal progenitors [33, 34]. In this study, the macrophage response to Plasma and UV treatment was investigated by investigating their Macrophage activation.

To this aim, RAW 264.7 cells were culture for 5 days on different samples (4 samples from each sub-group). IL-1; IL-6; TNFα and TGFβ were analyzed.

RNA extraction and real-time PCR analysis

Total RNA was extracted using PureLink RNA Mini Kit (Ambion, Life Technologies Italy). For quantitative real-time polymerase chain reaction (qRT-PCR), 0.3 μg total RNA was transcribed into complementary DNA by MultiScribe® Reverse Transcriptase (High-Capacity cDNA Reverse Transcription Kit, Thermo Fisher Scientific) and PCR analysis was then assessed using TaqMan probes from Roche. *Transcript* abundance, normalized to 18s mRNA expression, is expressed as a fold increase over a calibrator sample. qRT-PCR was performed on a 7900HT Fast Real-Time PCR System (Applied Biosystems, Life Technologies Italy). (Petrillo at al. 2018) Specific primers and probes were designed using the Universal Probe Library - Assay Design Center - Roche Life Science software.

Osteogenic differentiation

To induce osteogenic differentiation, D1 cells were cultured in osteogenic media by supplementing the normal culture medium with 10 mM glycerophosphate and 50 ng/mL ascorbic acid.

The osteogenic differentiation was evaluated measuring transcript level of RUNX2 and Collagen type 1 at 3, 7 days by using qPCR. Moreover, Alkaline Phosphatase Activity and calcium deposition were measured respectively at 3, 7 and 21 days.

Alkaline Phosphatase Activity

Alkaline Phosphatase Activity (ALP) was determined colorimetrically and assessed at day 7. Cells were lysed with 0.05% Triton X-100 and incubated with the reagent solution containing phosphatase substrate (Sigma-Aldrich, Milan, Italy) at 37 °C for 15 min. Alkaline phosphatase values were determined (OD 405 nm).

Alizarin Red S quantification

The extracellular matrix calcification was quantified by Alizarin Red staining. At day 21 cells were first incubated in a solution of 40 mM Alizarin Red (pH 4.2) and subsequently lysed with acetic acid. Absorbance of the lysates was finally measured at 405 nm.

Surface analysis

Samples were washed in PBS, fixed in a mixture of 2% formaldehyde and 2% glutaraldehyde in 0.15 M sodium cacodylate buffer, then dehydrated in a graded series of ethanol solutions (70%, 80%, 95% ethanol 10 min and twice in 100% ethanol 15 min) and subsequently critical point dried in a CPD 030 unit (Balzers Union, Liechtenstein). Samples were mounted on stubs using double-sided adhesive carbon disks and gold coated in an Emitech K550 (Emitech Ltd., Ashford, Kent, UK). Gold sputtered samples were analyzed with a Dualbeam FIB/SEM Helios Nanolab 600 microscope (FEI, Hillsboro, USA), an instrument that combines an electron beam (SEM column) with a focused gallium ion beam (FIB column), oriented at 52° and focusing on the same area of the specimen. Samples were examined by using the field emission SEM column of the dualbeam FIB/SEM, with secondary electrons, an operating voltage ranging from 2 KV to 5 kV and an applied current of 0.17 nA or 0.34 nA [35, 36]. The evaluation of graft surfaces was carried out with 110, 500, 1000, 2000, 5000 times magnification.

Statistical analysis

Differences between groups were analyzed using the ordinary one-way ANOVA with the Tukey's multiple comparison test and Student t test by using GraphPad Prism software (GraphPad Software,

Inc., La Jolla, CA, USA). All of the statistical comparisons were conducted with a 0.05 level of significance.

Results

Effect of experimental treatments on osteoblast adhesion on graft materials

As reported in Tables 1 and 2, plasma treatment significantly increased the level of cell adhesion on all tested graft surfaces (**Fig. 3**). Interestingly, UV treatment did not statistically significantly influence cell adhesion.

Effect of experimental treatments on osteoblast proliferation

As outlined in Tables 3 and 4, no statistically significant difference in cell proliferation was observed 72h following treatment among PAT, UV and controls in any of the tested parameters (**Fig. 4**).

Effect of experimental treatments on macrophage activation

In order to evaluate macrophage activation IL-1, IL-6, TNFα and TGFβ were analyzed on RAW 264.7 cells growth on different graft materials in different conditions. As reported in figure 5 no significant differences were observed among different conditions except for IL-6 on MG-HA ctrl vs. MG-HA Plasma treatment. On the other hand, it is possible to appreciate a slight trend of increase of transcript levels of IL-1 and IL-6 in plasma treated grafts compared to their control conditions. (**Fig. 5**).

Effect of experimental treatments on osteogenic differentiation.

To understand whether PAT and UV treatments were able to affect MSC differentiation, the transcription levels of two very well-known markers of osteodifferentiation (RUNX2 and Collagen type-I) 3 and 7 days after osteogenic induction were analyzed.

As shown in **figure 6 A, B**, only PAT treatment was able to induce osteogenic differentiation in all considered condition at 3 days. However, these differences were not observed after 7 days.

This behavior might suggest a role in early osteoinduction.

To further address this phenomenon, the activity of Alkaline Phosphatase at 7 days was investigated. As shown in **figure 7 A** both PAT and UV treatment failed to exert a significant different compared to control conditions.

The calcium deposition using Alizarin Red S staining 21 days after osteoinduction was then analyzed. The qualitative (**Fig. 7 B**) and quantitative (**Fig. 7 C**) results failed to show any difference in treated samples with both PAT and UV.

Biomaterial Topography following experimental treatments

As highlighted in Figure 8, the morphological analysis of Mg-E-HAP samples showed no obvious differences between the treated (UV and Plasma) and untreated material as, in all three cases, the specimens appeared rather homogeneous and made of nanoparticles with a diameter ranging from 40nm to 80nm.

Characterization of BCP compounds revealed that, while treatment with ultraviolet light failed to induce morphological alterations, treatment with Argon plasma caused some degree of modification to the nanoparticle shapes as they exhibit a polygonal shape that was completely different when compared to the more rounded appearance of the particles found in UV-treated and control samples. Moreover, after plasma treatment, the nanoparticles were greatly increased in size (roughly six times the volume of the UV-treated and untreated materials) and were often partially fused creating clusters of various dimensions.

Plasma treatment on cortical bone proved to effectively cause a morphological alternation consisting of increased roughness of the bone surface due to the formation of cavities and porosities that were otherwise undetectable on the UV-treated and untreated tissues. On the contrary, when applied to trabecular bones, the plasma treatment did not seem to influence the morphology of the samples that remained identical to the ones observed in the control sample. Both Calcium Phosphate and hydroxyapatite samples seem to be suitable for the proliferation and colonization of bone cells; in fact, osteoblasts adhered to the sample surface, appearing evenly distributed, and showed a spread morphology with evidence of cell protrusions.

Discussion

The results from the present study have shown that treatment with Argon plasma increased statistically significantly osteoblast adhesion on all four evaluated bone grafting materials, however no differences in osteoblast proliferation was observed. Most importantly, treatment with Argon plasma did not elicit any differences in macrophage number and it may therefore be expected that a potential inflammatory reaction caused by Argon plasma is low. Moreover, this work also suggested a role in early osteoinduction. The material topography remained almost unaltered suggesting the safety of this treatment modality in terms of biological effects and material integrity. On the contrary, UV light treatment failed to attain any effects (neither positive nor negative) on the properties in terms of biological responses or surface modification of any of the four tested grafting materials.

The present study was carefully designed to estimate the effect of Argon plasma on the osteoconductive potential of frequently utilized bone grafts by measuring osteoblast adhesion and proliferation on graft particles, as well as the effects of this treatment on macrophage viability and biomaterial topography. The design of the present study was based on the results of a previous experiment in murine cells which demonstrated enhanced cell response and protein adsorption on the tested surfaces following PAT [28].

To increase the reliability of the present study, a three-dimensional culture system (bioreactor) was utilized as opposed to a 2D culture system to better simulate physiological conditions. The two osteoblast cell lines were MG-63 and SaOs-2 offering reproducibility as previously discussed [37]. The former cell type represents an immature osteoblast phenotype, while the latter displays a mature osteoblast phenotype. SaOs-2 cells share with primary human mesenchymal cells a similar expression profile of chemokines, cytokines and growth factors [33], likewise both produce bone-like extracellular matrix. In the present study it was found that cell proliferation demonstrated a saturation effect after 72h due to the small surface of the experimental graft disks. This space limitation restricted the number of adherent cells/mm^2, which was in line with previously published data on titanium disks [38, 39]. On the other hand, macrophages did not seem to be as sensitive towards PAT or UV treatment pointing to the biological safety of these investigated treatments.

In the present work, plasma of Argon was demonstrated to positively influence the early osseo-differentiation of mesenchymal stem cells, although this effect seemed abolished when longer time points were considered. This difference could be related to the effect observed in cell adhesion. For a better comprehension of this phenomenon further studies using animal models are required. Indeed, in a more complex environment this early osteoinduction could achieve promising longitudinal outcomes.

In the present study, different graft materials were analyzed and activated through PAT, which allowed, at least, 30% higher cell adhesion on all bone grafting material surfaces, independently of the biomaterial type. It is conceivable that PAT activation of the biomaterial surface increased the surface energy and hydrophilicity, thus improving the adsorption of bone attractant factors such as fibronectin, vitronectin, actin, vinculin as previously reported [28]. These proteins provide mechanical attachment sites for the extracellular matrix, which are mandatory for cell adhesion [40]. Moreover, these findings suggest that PAT also increased the surface properties of the biomaterial, as it was also shown to favor an increase in osteoblast adhesion in the present study. However, the different structural characteristics of the investigated bone grafts need also to be considered when interpreting the results, and might present a potential subject of future research aiming to clarify of the exact impact of PAT on surface-related factors.

Interestingly, the present data are not in accordance with a previously published study by Beutel [41]. In fact, this study reported in an animal model that TCP activated by Argon plasma failed to show any statistically significantly higher bone regeneration compared to an untreated graft material. It may therefore be speculated that this difference in outcomes may be dependent on not only the material surface but also on the type of used reactor. While in the present study the plasma was created in a vacuum, the bioactivation in the study by Beutel was created using a plasma beam which works at atmospheric pressure. In fact, as demonstrated by Moisan [24] and Duske [22], the effect of the plasma is associated with several factors: the gas utilized, the time of exposure, the power and the pressure.

On the other hand, irrespectively to the material analyzed, the second test group irradiated by UV, which was demonstrated to increase the surface energy on titanium surfaces [42], failed to show

any significant effect on the graft material samples. This might be related to the fact that UV was able to activate only metal atoms, as documented by Hashimoto [43].

It should be highlighted that, as demonstrated by the SEM analysis, both tested treatments only minimally affected the microscopic structure of all tested graft materials, including the collagen portion of the xenogenic materials. This minimal topographic modification might be due to the temperature/pressure increasing during the plasma process. However, these minor topographic modifications did not hinder the biologic properties of the grafting materials.

One limitation of the present study is related to the difficulties of an *in vitro* model to simulate *in vivo* conditions where a great number of heterogeneous proteins interact simultaneously. Additionally, in the present study, a bi-dimensional analysis was performed which cannot assess tri-dimensional interactions between osteogenic cells and scaffolds.

Nevertheless, the present findings are encouraging and point to the potential biologic value of the plasma argon modality. Thus, further *in vitro* studies analyzing the tridimensional interactions between scaffolds and cells followed by preclinical and clinical testing are warranted in order to evaluate the potential clinical relevance and future safety of this method.

Conclusion

Within their limitations, the present results suggest that treatment of various bone grafting materials with PAT appears to enhance the osteoconductivity of bone substitutes by increasing cell adhesion and proliferation without affecting, at the same, time the number of adherent macrophages (cells known to promote and sustain inflammatory reactions).

Acknowledgements

Authors highly appreciated the skills and commitment of Dr. Audrenn Gautier in the supervision of the study and Dr. Henry Canullo for the scientific support.

Conflict of Interest: All authors explicitly declare that they have no conflict of interest.

Funding: the study was self-supported

Ethical approval: The study is an in vitro study. All procedures performed in studies involving human participants were in accordance with the ethical standards of the institutional and/or national research committee and with the 1964 Helsinki declaration and its later amendments or comparable ethical standards.

Informed consent: Informed consent was obtained from all individual participants included in the study.

Refence list

1. Sculean A, Chapple IL, Giannobile WV. (2015) Wound models for periodontal and bone regeneration: the role of biologic research. *Periodontol 2000*, *68*(1), pp.7-20.
2. Sanz-Sánchez I, Ortiz-Vigón A, Sanz-Martín I, Figuero E, Sanz, M. (2015) Effectiveness of Lateral Bone Augmentation on the Alveolar Crest Dimension: A Systematic Review and Meta-analysis. J Dent Res. 94: 128S-42S.
3. Sanz M, Vignoletti F. (2015) Key aspects on the use of bone substitutes for bone regeneration of edentulous ridges. Dent Mater. *31*(6), pp.640-647.
4. Araujo MG, Lindhe J. (2009) Ridge preservation with the use of Bio-Oss collagen: a 6-month study in the dog. Clin Oral Implants Res;20(5):433–40.
5. Cornelini R, Cangini F, Martuscelli G, Wennstrom J. (2004) Deproteinized bovine bone and biodegradable barrier membrane to support healing following immediate placement of transmucosal implants: a short-term controller clinical trial. Int J Periodontics Restorative Dent. 24: 555–563.
6. Chen ST, Darby IB, Reynolds EC. (2007) A prospective clinical study of non-submerged immediate implants. Clinical outcomes and esthetic results. Clin Oral Implants Res 18: 552–562.
7. Chen ST, Buser D. (2014) Esthetic outcomes following immediate and early implant placement in the anterior maxilla—a systematic review. Int J Oral Maxillofac Implants:186–215.
8. Raghoebar, G.M., Louwerse, C., Kalk, W.W. & Vissink, A. (2001) Morbidity of chin bone harvesting. Clinical Oral Implants Research 12: 503–507.
9. Lambert F, Bacevic M, Layrolle P, Schupbach P, Drion P, Rompen E. (2017) Impact of biomaterial microtopography on bone regeneration: comparison of three hydroxyapatites. Clin Oral Implants Res 28, , e201–e207
10. Clementini, M., Morlupi, A., Canullo, L., Agrestini, C, Barlattani, A. (2012) Success rate of dental implants inserted in horizontal and vertical guided bone regenerated areas: a systematic review. Int J Oral Maxillofac Implants. 41(7):847-852.
11. Thoma DS, Zeltner M, Hüsler J, Hämmerle CH & Jung RE (2015) Supplement Working Group 4 - EAO CC 2015 Short implants versus sinus lifting with longer implants to restore the posterior maxilla: a systematic review. Clin Oral Implants Res 26: 154-169.

12. Cortellini P, Tonetti MS. (2015). Clinical concepts for regenerative therapy in intrabony defects. *Periodontol 2000*, *68*(1), pp.282-307.
13. Trombelli L. (2005) Which reconstructive procedures are effective for treating the periodontal intraosseous defect? *Periodontol 2000*, *37*(1), pp.88-105.
14. Sculean A, Nikolidakis D, Schwarz F. (2008) Regeneration of periodontal tissues: combinations of barrier membranes and grafting materials - biological foundation and preclinical evidence: a systematic review. J Clin Periodontol.35 (8 Suppl): 106-116.
15. Fehrer C, Brunauer R, Laschober G, Unterluggauer H, Reitinger S, Kloss F, Gülly C, Gaßner R, Lepperdinger G. (2007) Reduced oxygen tension attenuates differentiation capacity of human mesenchymal stem cells and prolongs their lifespan. *Aging cell*, *6*(6), pp.745-757.
16. García-Gareta E, Coathup MJ, Blunn GW. (2015) Osteoinduction of bone grafting materials for bone repair and regeneration. Bone; 81:112-21
17. Götz W, Reichert C, Canullo L, Jäger A, Heinemann F. (2012) Coupling of osteogenesis and angiogenesis in bone substitute healing - a brief overview. Ann Anat. 20;194(2):171-3.
18. Lambert F, Bacevic M, Layrolle P, Schüpbach P, Drion P, Rompen E. (2017) Impact of biomaterial microtopography on bone regeneration: comparison of three hydroxyapatites. Clin Oral Implants Res. Oct;28(10): e201-e207.
19. Parizek M, Slepickova Kasalkova N, Bacakova L, Svindrych Z, Slepicka P, Bacakova M, Lisa V, Svorcik V. (2013) Adhesion, growth, and maturation of vascular smooth muscle cells on low-density polyethylene grafted with bioactive substances. Biomed Res Int.37: 14-30.
20. Bacakova, L., Filova, E., Parizek, M., Ruml, T. & Svorcik, V. (2011) Modulation of cell adhesion, proliferation and differentiation on materials designed for body implants. *Biotechnol Adv* 29: 739-767.
21. Coelho PG, Giro G, Teixeira HS, Marin C, Witek L, Thompson VP, Tovar N, Silva NRF. (2012) Argon-based atmospheric pressure plasma enhances early bone response to rough titanium surfaces. J Biomed Mater Res A.100: 1901-1906.
22. Duske K, Koban I, Kindel E, Schröder K, Nebe B, Holtfreter B, Jablonowski L, Weltmann KD, Kocher T. (2012). Atmospheric plasma enhances wettability and cell spreading on dental implant metals. *J Clin Period* 39: 400-407.
23. Swart KM, Keller JC, Wightman JP, Draughn RA, Stanford CM, Michaels CM. (1992) Short-term plasma-cleaning treatments enhance in vitro osteoblast attachment to titanium. *J Oral Impl* 18:130-137.

24. Pistilli R, Genova T, Canullo L, Faga MG, Terlizzi ME, Gribaudo G, Mussano F. (2018) Effect of Bioactivation on Traditional Surfaces and Zirconium Nitride: Adhesion and Proliferation of Preosteoblastic Cells and Bacteria. Int J Oral Maxillofac Implants. 33(6):1247-1254.
25. Moisan M, Barbeau J, Crevier MC, Pelletier J, Philip N, Saoudi N. (2002) Plasma sterilization. Methods and mechanisms. Pure Ap Chem; 74: 349–358
26. Canullo L, Micarelli C, Lembo-Fazio L, Iannello G, Clementini M. (2014) Microscopical and microbiologic characterization of customized titanium abutments after different cleaning procedures. Clin Oral Implants Res.;25(3):328-336.
27. Zhao G, Schwartz Z, Wieland M, Rupp F, Geis-Gerstorfer J, Cochran DL, Boyan BD. (2005). High surface energy enhances cell response to titanium substrate microstructure. J Biomed Mater Res A. 74: 49-58.
28. Canullo L, Genova T, Naenni N, Masuda K, Mussano F. (*2018)* Plasma of argon enhances the adhesion of murine. *Ann Anat, 218:265-270*
29. Genova T, Pesce P, Mussano F, Tanaka K, Canullo L. (2019) The influence of bone-graft biofunctionalization with plasma of argon on bacterial contamination. J Biomed Mater Res A. 107(1):67-70
30. Aita H, Att W, Ueno T, Yamada M, Hori N, Iwasa F, Tsukimura N, Ogawa T. (2009) Ultraviolet light-mediated photofunctionalization of titanium to promotehuman mesenchymal stem cell migration, attachment, proliferation and differentiation. Acta Biomater. 5(8):3247–3257
31. Mussano F, Genova T, Verga Falzacappa E, Scopece P, Munaron L, Rivolo P, Mandracci P, Benedetti A, Carossa S, Patelli, A. (2017) In vitro characterization of two different atmospheric plasma jet chemical functionalizations of titanium surfaces. Appl. Surf. Sci., 409, 314–324.
32. Mussano F, Genova T, Munaron L, Petrillo S, Erovigni F, Carossa S. (2016) Cytokine, chemokine and growth factor profile of platelet-rich plasma. *Platelets*, *27*, 467–471
33. Mussano F, Genova T, Corsalini M, Schierano G, Pettini F, Di Venere D, Carossa S. (2017) Cytokine, Chemokine, and Growth Factor Profile Characterization of Undifferentiated and Osteoinduced Human Adipose-Derived Stem Cells. *Stem Cells Int*. 25: 1–11,
34. Miron RJ, Bosshardt DD. (2016) OsteoMacs: Key players around bone biomaterials. *Biomaterials* 82: 1-19.

35. Schierano G, Mussano F, Faga MG, Menicucci G, Manzella C, Sabione C, Genova T, Degerfeld MM, Peirone B, Cassenti A, Cassoni P, Carossa S. (2015) An Alumina Toughened Zirconia Composite for Dental Implant Application: In Vivo Animal Results. *Biomed Res. Int. 20*, 1–9.
36. Canullo L, Genova T, Mandracci P, Mussano F, Abundo R, Fiorellini J. (2017) Morphometric Changes Induced by Cold Argon Plasma Treatment on Osteoblasts Grown on Different Dental Implant Surfaces. *Int. J. Period Rest Dent. 37*, 541–548.
37. Genova T, Munaron L, Carossa S, Mussano F. (**2016)** Overcoming physical constraints in bone engineering: the importance of being vascularized. *J. Biomater. Appl.*, *30*, 940–951,
38. Canullo L, Cassinelli C, Götz W, Tarnow D. (2013) Plasma of argon accelerates murine fibroblast adhesion in early stages of titanium disk colonization. *Int J Oral Maxillofac Impl*. 28: 957–962.
39. Canullo L, Genova T, Tallarico M, Gautier G, Mussano F, Botticelli, D. (2016) Plasma of Argon affects the earliest biological response of different implant surfaces: an in vitro comparative study. *J Dent Res*. 95: 566-73
40. Großner-Schreiber B, Herzog M, Hedderich J, Duck A, Hannig M, Griepentrog M. (2006) Focal adhesion contact formation by fibroblasts cultured on surface modified dental implants: an in vitro study. Clin Oral Implants Res. 17: 736–745
41. Beutel BG, Danna NR, Gangolli R, Granato R, Manne L, Tovar N Coelho PG. (2014) Evaluation of bone response to synthetic bone grafting material treated with argon-based atmospheric pressure plasma. Mater Sci Eng C Mater Biol Appl. 45: 484-490.
42. Iwasa F, Hori N, Ueno T, Minamikawa H, Yamada M, Ogawa T. (2010) Enhancement of osteoblast adhesion to UV-photofunctionalized titanium via an electrostatic mechanism Biomaterials 31 2717–2727
43. Hashimoto K, Irie H, Fujishima A. (2005) TiO2 Photocatalysis: A Historical Overview and Future Prospects. Jap J Appl Physics. 44,12: 8269–8285

Tables

MG63 Adhesion												
BCP CTRL	**BCP PLASMA**	**BCP UV**	**MG-HA CTRL**	**MG-HA PLASMA**	**MG-HA UV**	**Cancellous BM CTRL**	**Cancellous BM PLASMA**	**Cancellous BM UV**	**Cortical BM CTRL**	**Cortical BM Plasma**	**Cortical BM UV**	
51.75	112.75	62.75	40	95	54.5	52.5	178.5	70.5	99	200.25	118.25	**mean**
4.25	17.259	5.006	4.564	9.5655	12.841	10.507	9.869	15.3106	4.654	14.55	25.240	**err.st.**

Tab.1 MG63 adhesion, data expressed as cell number/field.

Saos-2 Adhesion												
BCP CTRL	**BCP PLASMA**	**BCP UV**	**MG-HA CTRL**	**MG-HA PLASMA**	**MG-HA UV**	**Cancellous BM CTRL**	**Cancellous BM PLASMA**	**Cancellous BM UV**	**Cortical BM CTRL**	**Cortical BM Plasma**	**Cortical BM UV**	
49.5	100	64.25	60.25	122.5	65.5	40.5	148.25	51	79	160.5	94.5	**mean**
10.851	7.7028	16.079	8.9477	4.5	13.8413	10.77419	12.931	19.8871818	15.28	9.36	13.357	**err.st.**

Tab.2 Saos-2 adhesion, data expressed as cell number/field.

MG63 proliferation at 72h												
BCP CTRL	**BCP PLASMA**	**BCP UV**	**MG-HA CTRL**	**MG-HA PLASMA**	**MG-HA UV**	**Cancellous BM CTRL**	**Cancellous BM PLASMA**	**Cancellous BM UV**	**Cortical BM CTRL**	**Cortical BM Plasma**	**Cortical BM UV**	
6305	6917	7505.2	5056.5	4882.5	4635	10002.75	9579	9280.25	8673	9328.25	8634.25	**mean**
318.46	757.32	609.4	722.36	548.687	616.564	619.934	978.684	911.080	436.5	720.252	593.03	**err.st.**

Tab. 3 MG63 proliferation, data expressed as relative luminescent units.

Saos-2 proliferation at 72h												
BCP CTRL	**BCP PLASMA**	**BCP UV**	**MG-HA CTRL**	**MG-HA PLASMA**	**MG-HA UV**	**Cancellous BM CTRL**	**Cancellous BM PLASMA**	**Cancellous BM UV**	**Cortical BM CTRL**	**Cortical BM Plasma**	**Cortical BM UV**	
4465.75	4535.75	3849.2	3735.75	3597.75	3423.5	8182.75	8516.75	7897.25	5608.25	6070.5	6398	**mean**
717.616	807.7253	685.70	93.30	758.2216	455.9	997.899	1236.523	1165.79	720.40	572.7	1128.60	**err.st.**

Tab.4 Saos-2 proliferation, data expressed as relative luminescent units.

RUNX2 3 days												
BCP CTRL	**BCP PLASMA**	**BCP UV**	**MG-HA CTRL**	**MG-HA PLASMA**	**MG-HA UV**	**Cancellous BM CTRL**	**Cancellous BM PLASMA**	**Cancellous BM UV**	**Cortical BM CTRL**	**Cortical BM Plasma**	**Cortical BM UV**	
1,00	1,78	1,14	1,18	2,11	1,34	2,49	2,94	2,23	1,81	2,62	2,22	**mean**
0,12	0,23	0,35	0,32	0,08	0,40	0,25	0,14	0,16	0,21	0,12	0,21	**err.st.**

Tab.5 MSC expression of RUNX-2 at 3 days, data expressed as RQ.

RUNX2 7 days												
BCP CTRL	BCP PLASMA	BCP UV	MG-HA CTRL	MG-HA PLASMA	MG-HA UV	Cancellous BM CTRL	Cancellous BM PLASMA	Cancellous BM UV	Cortical BM CTRL	Cortical BM Plasma	Cortical BM UV	
2,78	2,88	2,69	2,90	2,73	2,77	2,84	2,79	2,70	2,73	2,69	2,59	**mean**
0,45	0,22	0,42	0,38	0,27	0,55	0,28	0,42	0,40	0,39	0,52	0,69	**err.st.**

Tab.6 MSC expression of RUNX-2 at 7 days, data expressed as RQ.

COL1A 3 days												
BCP CTRL	BCP PLASMA	BCP UV	MG-HA CTRL	MG-HA PLASMA	MG-HA UV	Cancellous BM CTRL	Cancellous BM PLASMA	Cancellous BM UV	Cortical BM CTRL	Cortical BM Plasma	Cortical BM UV	
1,00	1,74	1,32	1,13	2,22	1,36	2,43	3,30	2,53	2,71	3,04	2,40	**mean**
0,16	0,25	0,10	0,32	0,07	0,27	0,46	0,29	0,17	0,21	0,37	0,26	**err.st.**

Tab.7 MSC expression of Collagen Type 1 at 3 days, data expressed as RQ.

COL1A 7 days												
BCP CTRL	BCP PLASMA	BCP UV	MG-HA CTRL	MG-HA PLASMA	MG-HA UV	Cancellous BM CTRL	Cancellous BM PLASMA	Cancellous BM UV	Cortical BM CTRL	Cortical BM Plasma	Cortical BM UV	
3,72	3,38	3,22	3,14	3,28	3,38	5,32	5,22	5,11	4,94	4,71	5,23	**mean**
0,45	0,50	0,43	0,16	0,59	0,38	0,50	0,81	0,80	0,93	1,03	0,82	**err.st.**

Tab.8 MSC expression of Collagen Type 1 at 7 days, data expressed as RQ.

ALP Activity Assay												
BCP CTRL	BCP PLASMA	BCP UV	MG-HA CTRL	MG-HA PLASMA	MG-HA UV	Cancellous BM CTRL	Cancellous BM PLASMA	Cancellous BM UV	Cortical BM CTRL	Cortical BM Plasma	Cortical BM UV	
0,43	0,40	0,43	0,28	0,31	0,33	0,54	0,58	0,54	0,63	0,62	0,60	**mean**
0,03	0,07	0,07	0,04	0,05	0,08	0,08	0,11	0,07	0,10	0,07	0,09	**err.st.**

Tab.9 ALP Activity assay at 7 days, data expressed as OD 405 nm.

Alizarin Red S Quantification											
BCP PLASMA	BCP UV	MG-HA CTRL	MG-HA PLASMA	MG-HA UV	Cancellous BM CTRL	Cancellous BM PLASMA	Cancellous BM UV	Cortical BM CTRL	Cortical BM Plasma	Cortical BM UV	
0,56	0,61	0,61	0,77	0,74	0,75	1,67	1,71	1,60	1,41	1,38	**mean**
0,07	0,15	0,10	0,15	0,14	0,17	0,22	0,30	0,24	0,17	0,13	**err.st.**

Tab.10 Alizarin Red S Quantification at 21 days, data expressed as OD 405 nm.

Figure legend

Fig. 1: **Flow diagram** of the randomization sequence

Fig. 2: **Bioreactor chamber architecture**. Representation of the bioreactor used to culture MG63 and Saos-2. The bioreactor is composed by two chambers separated by a porous membrane. The graft material is kept in the upper chamber and it is properly perfused by culture media.

Fig. 3: **Cell adhesion.** Cell adhesion was evaluated on MG63 (A) and on Saos-2 (B) 15 min after seeding. The level of cell adhesion was measured counting the number of cellular nuclei stained with DAPI. Values represent mean ± SEM; for each graft material, the symbol (*) indicates a statistically significant difference with the relative control condition (CTRL), considering a p-value < 0.05.

Fig. 4: **Cell proliferation**. Cell proliferation was evaluated on MG63 (A) and on Saos-2 (B) 72h after seeding and keeping the graft materials in the bioreactor. The rate of cell proliferation was measured using CellTiter GLO (Promega). Values represent mean ± SEM.

Fig. 5: **Expression profile of IL-1 IL-1, IL-6, TNFα and TGFβ**. qRT-PCR analysis of IL-1, IL-6, TNFα and TGFβ performed on RAW 264.7 cells growth for 5 days on different graft materials in control condition, plasma treatment and UV treatment. Statistical analysis was performed using ordinary one-way ANOVA using Tukey's multiple comparison test. A p value >0.05 was considered significant. Values represent mean ± SEM.

Fig. 6: **Expression profile of RUNX-2 and Collagene Type 1.** qRT-PCR analysis of RUNX-2 (A) and Collagene Type 1 (B) performed on MSC growth in osteodifferentiating media for 3 and 7 days on different graft materials in control condition, plasma treatment and UV treatment. A p value >0.05 was considered significant. Values represent mean ± SEM.

Fig. 7: **ALP activity Mineralization**. Alkaline Phosphatase Activity (A), Alizarin red S (B,C) was determined and assessed respectively at 7 and 21 days after osteoinduction on different graft materials in control condition, plasma treatment and UV treatment. Statistical analysis was performed using ordinary one-way ANOVA using Turkey's multiple comparison test. A p value >0.05 was considered significant. Values represent mean ± SEM.

Fig. 8: Microscopic analysis of the surfaces pre- and post- treatments.

Fig.1

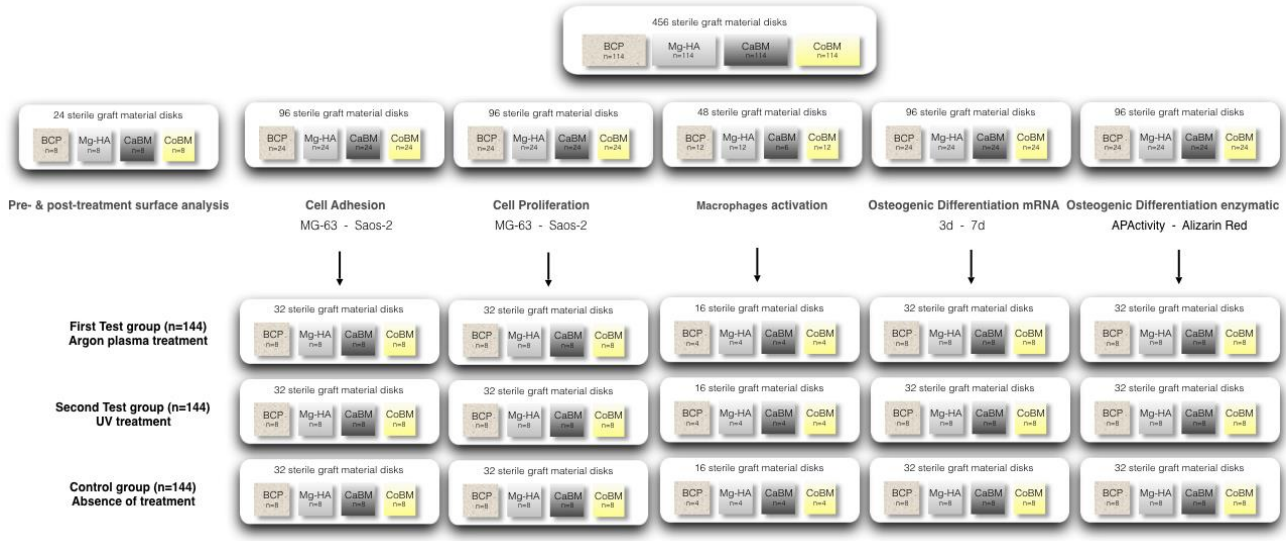

Fig.2

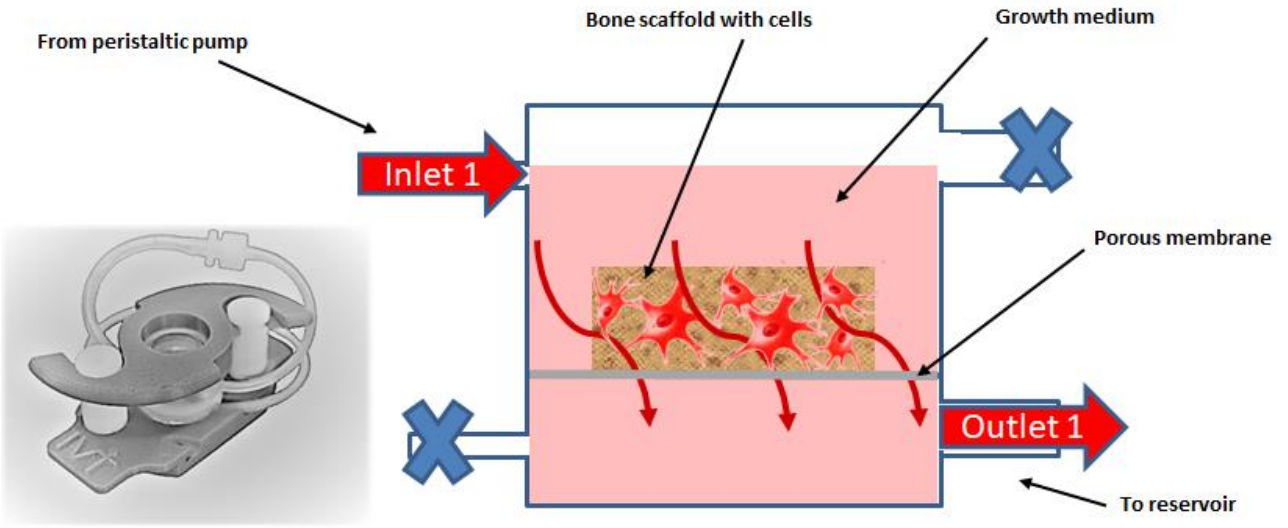

Fig.3

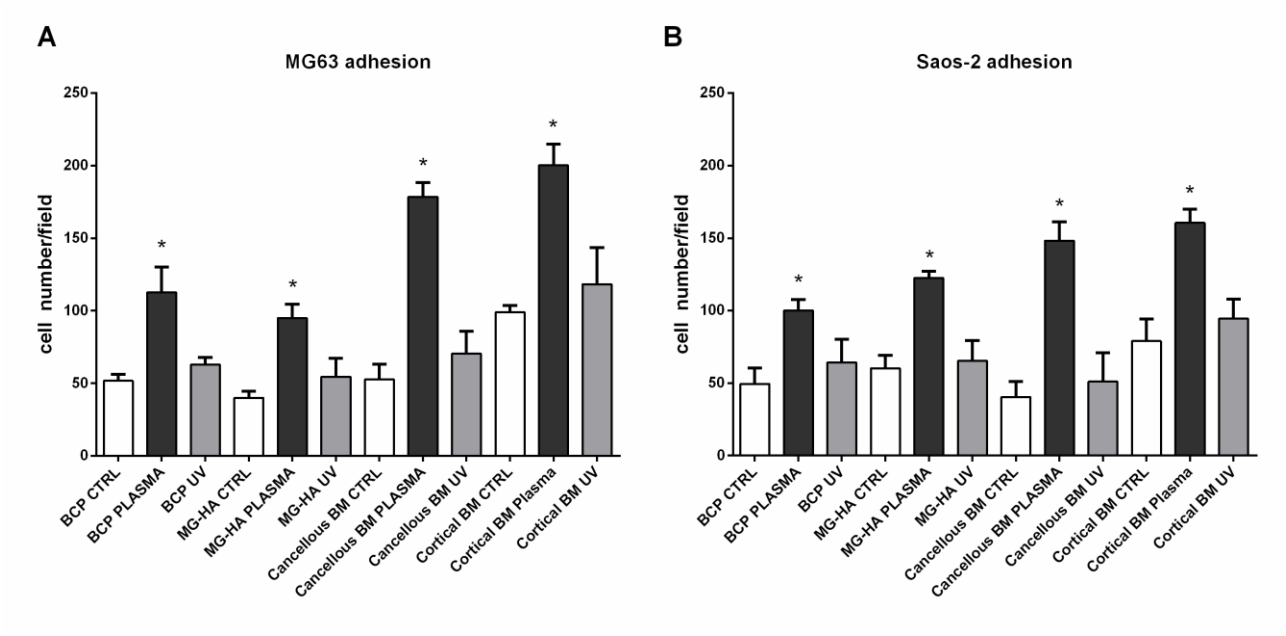
A
MG63 adhesion
cell number/field
250
200
150
100
50
0
*
BCP CTRL
BCP PLASMA
BCP UV
MG-HA CTRL
MG-HA PLASMA
MG-HA UV
Cancellous BM CTRL
Cancellous BM PLASMA
Cancellous BM UV
Cortical BM CTRL
Cortical BM Plasma
Cortical BM UV
B
Saos-2 adhesion
cell number/field
250
200
150
100
50
0
*
BCP CTRL
BCP PLASMA
BCP UV
MG-HA CTRL
MG-HA PLASMA
MG-HA UV
Cancellous BM CTRL
Cancellous BM PLASMA
Cancellous BM UV
Cortical BM CTRL
Cortical BM Plasma
Cortical BM UV

Fig.4

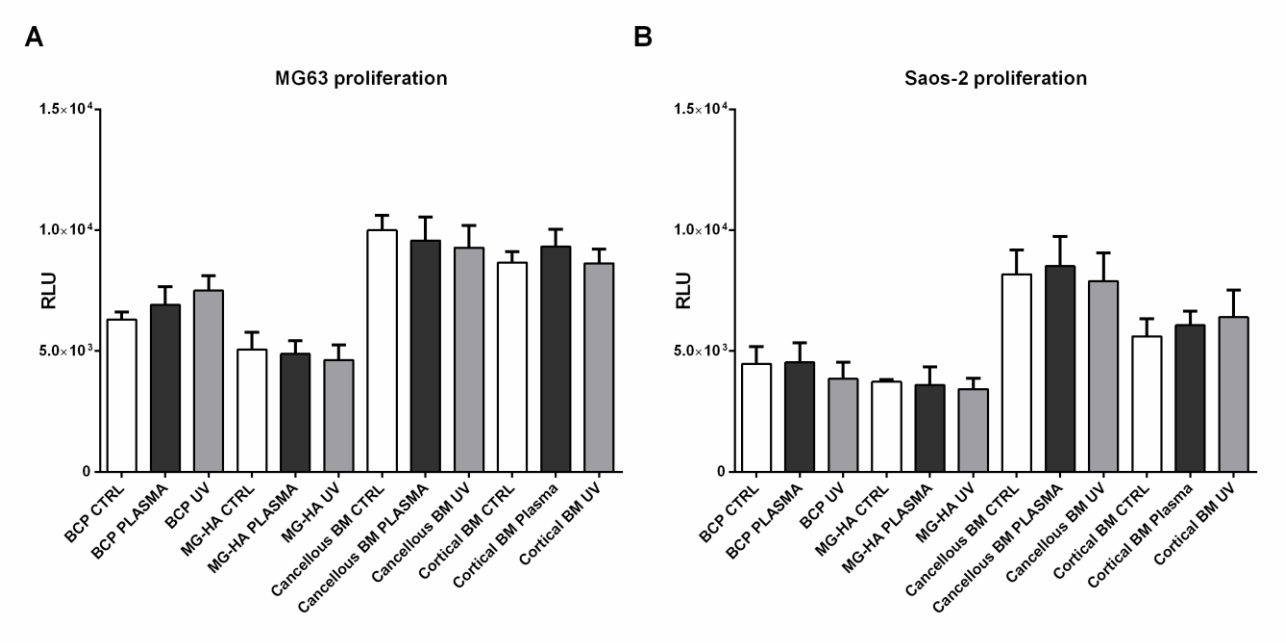
A
MG63 proliferation
RLU
1.5×10⁴
1.0×10⁴
5.0×10³
0
BCP CTRL
BCP PLASMA
BCP UV
MG-HA CTRL
MG-HA PLASMA
MG-HA UV
Cancellous BM CTRL
Cancellous BM PLASMA
Cancellous BM UV
Cortical BM CTRL
Cortical BM Plasma
Cortical BM UV
B
Saos-2 proliferation
RLU
1.5×10⁴
1.0×10⁴
5.0×10³
0
BCP CTRL
BCP PLASMA
BCP UV
MG-HA CTRL
MG-HA PLASMA
MG-HA UV
Cancellous BM CTRL
Cancellous BM PLASMA
Cancellous BM UV
Cortical BM CTRL
Cortical BM Plasma
Cortical BM UV

Fig.5

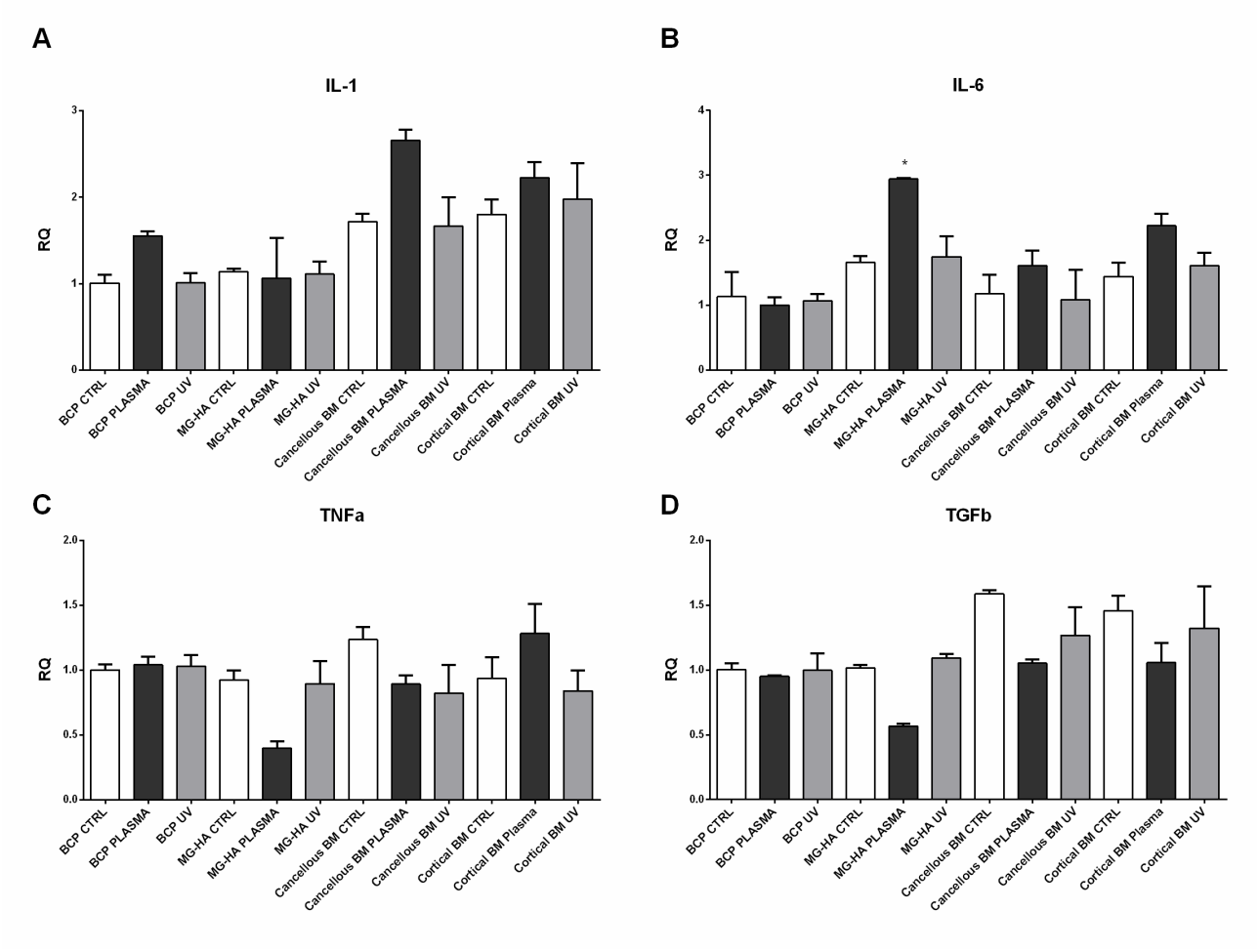
A
IL-1
RQ
B
IL-6
RQ
*
C
TNFa
RQ
D
TGFb
RQ
BCP CTRL
BCP PLASMA
BCP UV
MG-HA CTRL
MG-HA PLASMA
MG-HA UV
Cancellous BM CTRL
Cancellous BM PLASMA
Cancellous BM UV
Cortical BM CTRL
Cortical BM Plasma
Cortical BM UV

Fig.6

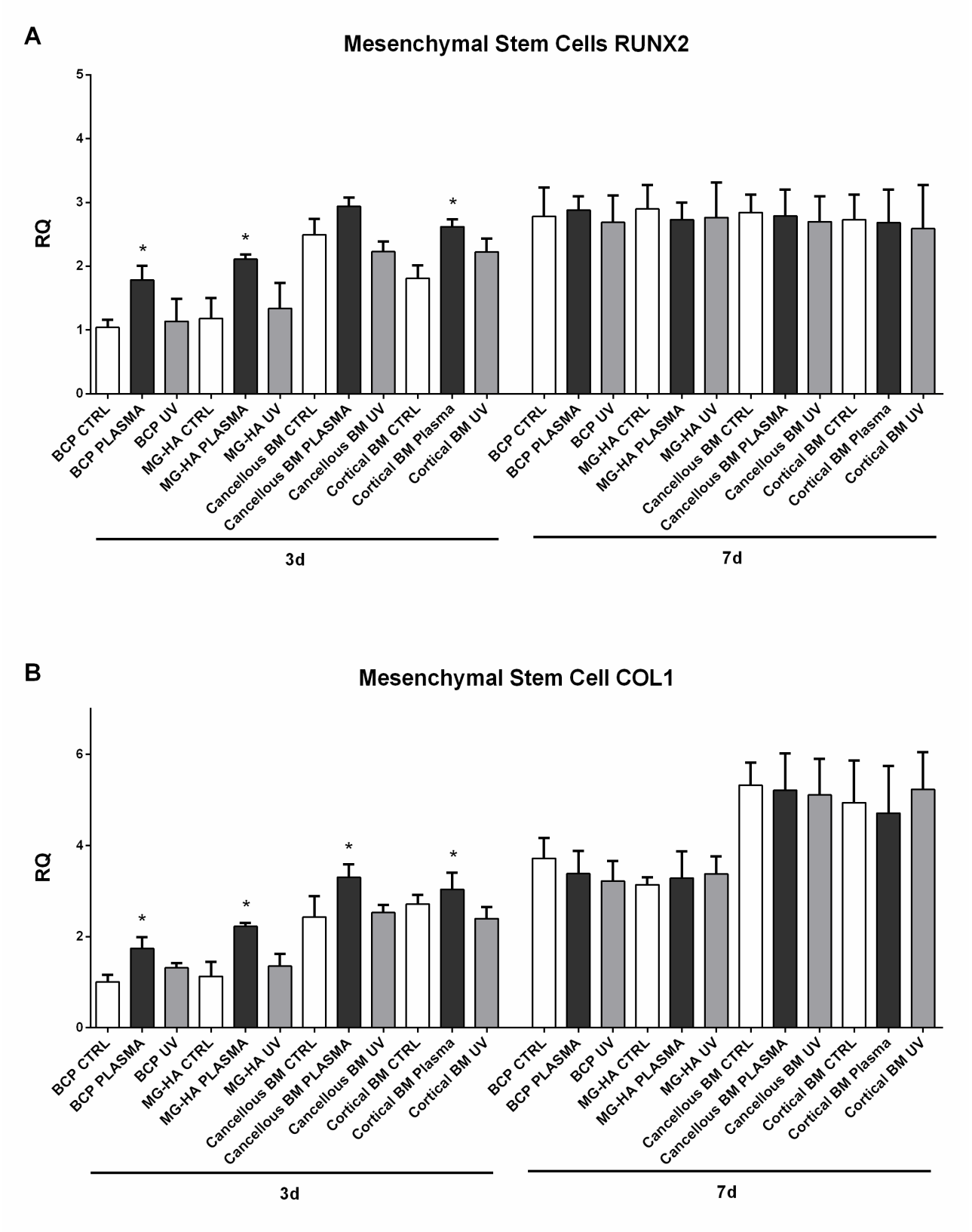
A
Mesenchymal Stem Cells RUNX2
RQ
0
1
2
3
4
5
*
*
*
BCP CTRL
BCP PLASMA
BCP UV
MG-HA CTRL
MG-HA PLASMA
MG-HA UV
Cancellous BM CTRL
Cancellous BM PLASMA
Cancellous BM UV
Cortical BM CTRL
Cortical BM Plasma
Cortical BM UV
3d
7d
B
Mesenchymal Stem Cell COL1
RQ
0
2
4
6
*
*
*
BCP CTRL
BCP PLASMA
BCP UV
MG-HA CTRL
MG-HA PLASMA
MG-HA UV
Cancellous BM CTRL
Cancellous BM PLASMA
Cancellous BM UV
Cortical BM CTRL
Cortical BM Plasma
Cortical BM UV
3d
7d

Fig.7

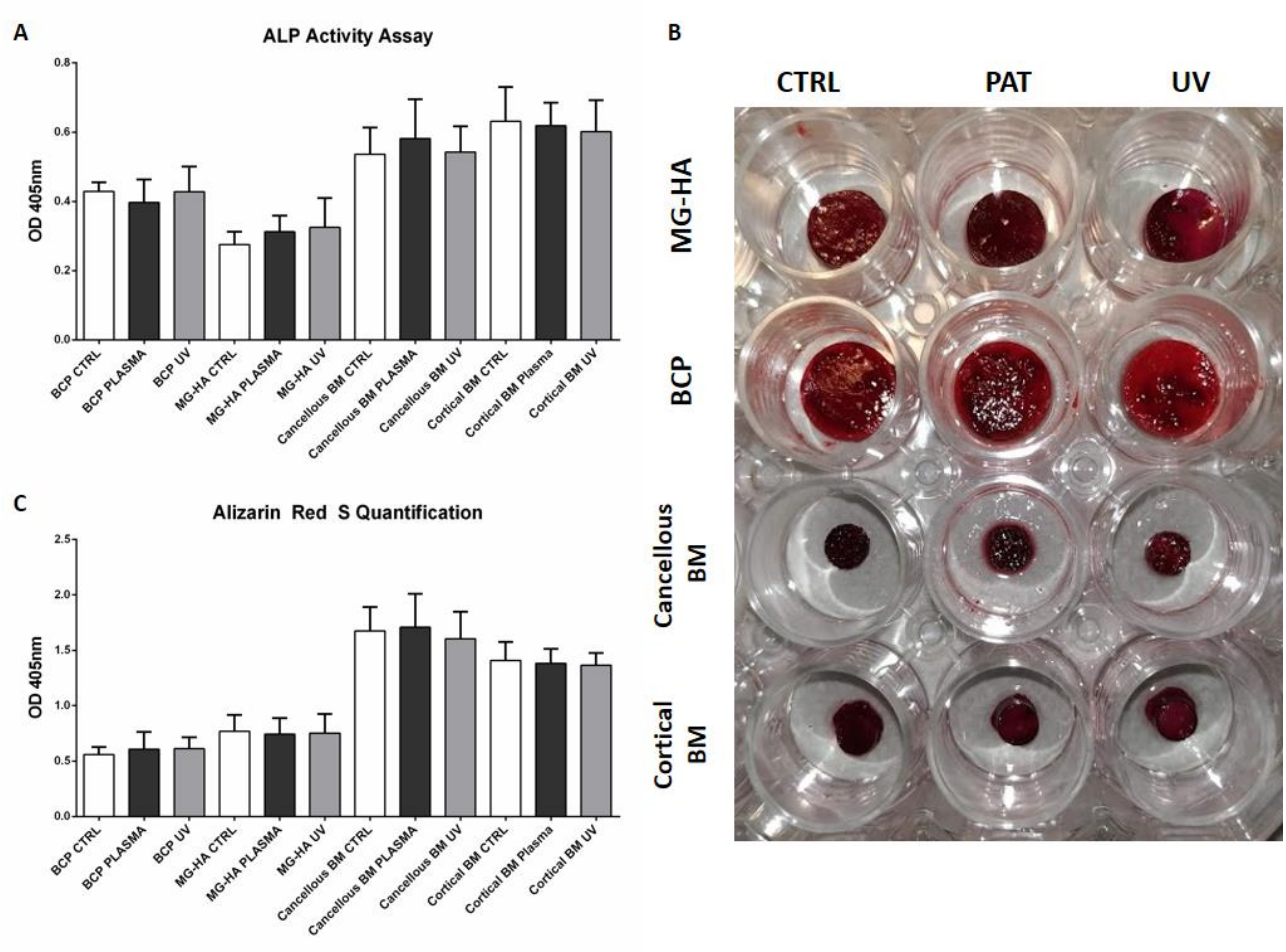
A
ALP Activity Assay
OD 405nm
0.0
0.2
0.4
0.6
0.8
BCP CTRL
BCP PLASMA
BCP UV
MG-HA CTRL
MG-HA PLASMA
MG-HA UV
Cancellous BM CTRL
Cancellous BM PLASMA
Cancellous BM UV
Cortical BM CTRL
Cortical BM Plasma
Cortical BM UV
B
CTRL
PAT
UV
MG-HA
BCP
Cancellous BM
Cortical BM
C
Alizarin Red S Quantification
OD 405nm
0.0
0.5
1.0
1.5
2.0
2.5
BCP CTRL
BCP PLASMA
BCP UV
MG-HA CTRL
MG-HA PLASMA
MG-HA UV
Cancellous BM CTRL
Cancellous BM PLASMA
Cancellous BM UV
Cortical BM CTRL
Cortical BM Plasma
Cortical BM UV

Fig.8